

## Conclusions

Since asymmetric bidentate ligands are able to coordinate in two different ways to the  $\text{Mo}_3\text{S}(\text{S}_2)_3$  core, the complexes with such ligands are of particular interest. The structure of the *msa* complex has been described previously.<sup>4</sup> It is noteworthy that, in the *msa* as well as in the *mbs* complex, the same arrangement of the ligands was found (cis position for the sulfur atoms with respect to  $\mu_3\text{-S}$ ). Both complexes were prepared by the same procedure starting from  $[\text{Mo}_3\text{S}(\text{S}_2)_3\text{Br}_6]^{2-}$ . Nothing is known about the mechanistic details of the ligand substitution; however, the exclusive formation of only one type of coordination indicates a highly selective process. We believe that the high coordination number of Mo favors a dissociative substitution mechanism. The facile dissociation of Br, also observed in the gaseous phase,<sup>10</sup> is in agreement with this assumption. A compilation of structural data about  $\text{Mo}_3\text{S}(\text{S}_2)_3$  complexes with either equal monodentate ligands or bidentate  $C_{2v}$  ligands revealed clearly a significant longer Mo–ligand bond for the trans position.<sup>5</sup> If we interpret this result as a trans effect of the  $\mu_3\text{-S}$  atom, it seems likely that the high selectivity can be explained by the following mechanism: (i) dissociation of a  $\text{Br}^-$  in trans position; (ii) attack of a deprotonated  $-\text{COO}^-$  group on Mo (with regard to this step, it is important to realize that the acidity of the SH group in acetonitrile is too low for significant deprotonation by  $\text{NEt}_3$ ); (iii) substitution of the second  $\text{Br}^-$  by the mercapto group; (iv) deprotonation of the coordinated mercapto group. It has already been shown that the Mo–S bond is quite inert.<sup>5</sup> Therefore, once the isomer is formed, it will keep its initial configuration.

The electrochemical studies demonstrate that in  $\text{Mo}_3\text{S}(\text{S}_2)_3$  complexes the disulfido groups and not Mo(IV) were reduced on the electrode surface. This result corresponds to the reactivity of  $\text{Mo}_3\text{S}(\text{S}_2)_3$  complexes with "chemical" reducing agents. As is well-known, these complexes degrade in the presence of cyanide or triphenylphosphine to  $\text{Mo}_3\text{S}_4$  derivatives.<sup>14</sup> In addition, it has

been shown recently that oxidizing agents attack selectively the terminal disulfido groups of  $[\text{Mo}_3\text{S}(\text{S}_2)_6]^{2-}$ .<sup>3,5</sup> Thus, as discussed previously, the  $\text{Mo}_3\text{S}(\text{S}_2)_3$  complexes are an illustrative model to show the different reactivity of coordinated disulfido groups. The stability of Mo(IV) against both reducing and oxidizing agents is quite remarkable. For *triangulo*- $\text{Mo}_3\text{S}_4$  complexes a reduction of Mo(IV) has been reported and complexes of the core  $\text{Mo}^{\text{IV}}_2\text{Mo}^{\text{III}}\text{S}_4$  and  $\text{Mo}^{\text{IV}}\text{Mo}^{\text{III}}_2\text{S}_4$  have been postulated.<sup>15</sup> According to the results presented in this study, the electron uptake of  $\text{Mo}_3\text{S}(\text{S}_2)_3$  complexes occurs obviously by the  $\sigma^*$  orbital of the disulfido group and is followed by the disruption of the S–S bond. Taking into account that coordinated ligands do not affect this reactivity, reduced species with an intact  $\text{Mo}_3\text{S}(\text{S}_2)_3$  core can hardly exist at all.

**Acknowledgment.** We thank Ruth Blumer and Dr. Heinz R uegger for the measurements of the NMR spectra, Dr. F. Behm for helpful advice, and Dr. R. Kissner and Dr. S. Wunderli for helpful discussions about the interpretation of the electrochemical measurements. The support of this work by the Swiss National Science Foundation is gratefully acknowledged.

**Registry No.**  $(\text{HNEt}_3)_2[\text{Mo}_3\text{S}_7(\text{mba})_3]$ , 129198-30-7;  $(\text{NEt}_4)_2[\text{Mo}_3\text{S}_7\text{Br}_6]$ , 127294-35-3;  $[\text{C}_{18}\text{H}_{30}\text{N}_3]_2[\text{Mo}_3\text{S}_7(\text{Hdba})_3]_3$ , 136061-36-4;  $(\text{HNEt}_3)_4[\text{Mo}_3\text{S}_7(\text{Hdsa})_2(\text{Hzdsa})]$ , 136061-34-2;  $[\text{Mo}_3\text{S}_7(\text{Hmsa})_3]^{2-}$ , 136172-03-7;  $[\text{Mo}_3\text{S}_7(\text{msa})_3]^{2-}$ , 129262-36-8;  $[\text{Mo}_3\text{S}_7(\text{mba})_3]^{2-}$ , 129262-31-3;  $[\text{Mo}_3\text{S}_7(\text{Hdba})_3]^{2-}$ , 136061-32-0;  $[\text{Mo}_3\text{S}_7(\text{Hdsa})_2(\text{H_2dsa})]^{4-}$ , 136061-31-9;  $[\text{Mo}_3\text{S}_7(\text{H_2dsa})_3]^{2-}$ , 136061-30-8; S, 7704-34-9; Hg, 7439-97-6.

**Supplementary Material Available:** Tables SI–SIV, listing crystallographic data, anisotropic displacement parameters, and bond distances and angles, and Figures S1–S3, showing the FAB<sup>+</sup> mass spectra of  $(\text{NEt}_4)_2[\text{Mo}_3\text{S}_7(\text{Hdba})_3]$  and  $(\text{HNEt}_3)_4[\text{Mo}_3\text{S}_7(\text{H_2dsa})(\text{Hdsa})_2]$  and a stereoview of the unit cell of  $(\text{HNEt}_3)_2[\text{Mo}_3\text{S}_7(\text{mba})_3]$ , respectively (10 pages); a table of calculated and observed structure factors (12 pages). Ordering information is given on any current masthead page.

(14) (a) M ller, A.; Reinsch, U. *Angew. Chem.* **1980**, *92*, 69. (b) Keck, H.; Kuchen, W.; Mathow, J.; Wunderlich, H. *Angew. Chem.* **1982**, *94*, 927. (c) Halbert, T. R.; McGauley, K.; Pan, W.-H.; Czernuszewicz, R. S.; Stiefel, E. I. *J. Am. Chem. Soc.* **1984**, *106*, 1849.

(15) (a) Wiegardt, K.; Herrmann, W.; M ller, A.; Eltzner, W.; Zimmermann, M. Z. *Naturforsch.* **1984**, *39B*, 876. (b) Shibahara, T.; Kuroya, H. *Polyhedron* **1986**, *5*, 357.

Contribution from the Dipartimento di Chimica Inorganica e Metallorganica e Centro CNR and Istituto di Chimica Strutturistica Inorganica, Universit  degli Studi di Milano, via G. Venezian 21, I 20133 Milano, Italy

## Reaction of Dioxygen with $[\text{Cu}(\text{dmpz})_n]$ ( $\text{Hdmpz} = 3,5\text{-Dimethylpyrazole}$ ). Crystal Structure, Reactivity, and Catalytic Properties of $[\text{Cu}_8(\text{dmpz})_8(\text{OH})_8]$

G. Attilio Ardizzoia,<sup>1a</sup> M. Angela Angaroni,<sup>1a</sup> Girolamo La Monica,<sup>\*1a</sup> Franco Cariati,<sup>1a</sup> Sergio Cenini,<sup>1a</sup> Massimo Moret,<sup>\*1b</sup> and Norberto Masciocchi<sup>1b</sup>

Received April 23, 1991

The species  $[\text{Cu}_8(\text{dmpz})_8(\text{OH})_8]$  (**2**) ( $\text{Hdmpz} = 3,5\text{-dimethylpyrazole}$ ) has been obtained by reacting  $[\text{Cu}(\text{dmpz})_n]$  (**1**) with  $\text{O}_2$  at atmospheric pressure and room temperature in wet solvents. Crystal data for  $[\text{Cu}_8(\text{dmpz})_8(\text{OH})_8] \cdot 2\text{C}_6\text{H}_5\text{NO}_2$  (22  C):  $a = 10.229$  (3)  ,  $b = 27.217$  (2)  ,  $c = 14.532$  (1)  ,  $\beta = 98.51$  (1)   with  $Z = 2$  in the space group  $P2_1/m$ .  $[\text{Cu}_8(\text{dmpz})_8(\text{OH})_8]$  consists of a discrete octameric molecule with a cyclic planar system of copper(II) atoms, bridged by OH and *dmpz* ligands, forming a molecule of toroidal shape; in the crystal, its cavity (viable diameter of ca. 6  ) contains crystallographically disordered, possibly water, molecules; in addition, fully ordered clathrated nitrobenzene molecules have been found between the octameric units. Complex **2** is catalytically active in the oxidation reactions of organic substrates such as triphenylphosphine, aromatic primary amines, dibenzylamine, and carbon monoxide, triphenylphosphine oxide, azobenzenes, *N*-benzylidenebenzylamine and carbon dioxide being respectively formed. Its reaction with  $\text{PPH}_3$  under an inert atmosphere gave 4 mol of  $\text{O}=\text{PPH}_3$  per mole of **2**, suggesting that **2** gives rise, in solution, to tautomeric species of the general formula  $[\text{Cu}_8(\text{dmpz})_8(\text{O})_x(\text{OH})_{8-2x}(\text{H}_2\text{O})_x]$  ( $x = 1\text{--}4$ ), which might behave as the active species. Complex **2** allowed also the stoichiometric oxidation of cyclohexyl isocyanide into the corresponding isocyanate in the absence or in the presence of  $\text{O}_2$ . The reaction of **2** with primary alcohols  $\text{R}'\text{OH}$  ( $\text{R}' = \text{Me}, \text{Et}, \text{Pr}^n$ , allyl) affords the octaalkoxo derivatives  $[\text{Cu}_8(\text{dmpz})_8(\text{OR}')_8]$  (**3**) whose formulation is suggested on the basis of analytical and spectroscopic data, as well as on chemical properties.

## Introduction

Polynuclear complexes are of interest because of their bonding and magnetic interactions and also because of their potential role

in catalysis.<sup>2</sup> The reaction of dioxygen with copper-containing compounds occurs in a large variety of important synthetic, in-

(1) (a) Dipartimento di Chimica Inorganica e Metallorganica e Centro CNR. (b) Istituto di Chimica Strutturistica Inorganica.

(2) (a) McKee, V.; Tandon, S. S. *J. Chem. Soc., Dalton Trans.* **1991**, 221. (b) Hoskins, B. F.; Robson, R.; Smith, P. *J. Chem. Soc., Chem. Commun.* **1990**, 488.

dustrial, and biological processes.<sup>3</sup> Moreover, binuclear bis( $\mu$ -hydroxo)-bridged complexes of almost all the transition metals have been prepared and their structures and chemistry thoroughly investigated.<sup>4</sup> Copper dimers having a single OH group as a bridging ligand have also been reported.<sup>4</sup>

As a part of a systematic study of the chemical properties of new and already known copper(I)-pyrazolate complexes, we recently reported the reactions of the polymeric Cu(I)-3,5-dimethylpyrazolate derivative,  $[\text{Cu}(\text{dmpz})]_n$  (**1**), with neutral ligands such as 1,10-phenanthroline and cyclohexyl isocyanide.<sup>5</sup>

In order to learn more about the chemistry of **1**, we decided to investigate its reaction with molecular oxygen. In most known cases, the reaction of dioxygen with Cu(I) complexes leads to the formation of oxo- and/or hydroxo-Cu(II) species resulting from the overall four-electron reduction and cleavage of the O-O bond of  $\text{O}_2$ .<sup>3</sup> For such species relatively few X-ray crystallographic structures have been reported.<sup>3</sup>

In this paper, we report the full structural characterization of the first example of an octanuclear copper(II)-hydroxo complex  $[\text{Cu}_8(\text{dmpz})_8(\text{OH})_8]$  (**2**), some reactions, and its catalytic properties in the selective oxidation reactions of some organic substrates. A brief account of this work appeared recently.<sup>6</sup>

### Experimental Section

Pyrazole, 3,5-dimethylpyrazole, cyclohexyl isocyanide and *p*-toluidine were used as supplied (Aldrich Chemical Co.); triphenylphosphine was recrystallized from methanol. Aniline and dibenzylamine were vacuum-distilled prior to use. Solvents were dried and distilled by standard methods.  $[\text{Cu}(\text{pz})]_n$  and  $[\text{Cu}(\text{dmpz})]_n$  (Hpz = pyrazole, Hdmpz = 3,5-dimethylpyrazole) were prepared according to literature procedures.<sup>7</sup>

Infrared spectra were recorded as Nujol mulls and KBr pellets on a JASCO FT-IR 5000 spectrometer; magnetic moments were determined according to Faraday's method by using a Cahn-Ventron magnetic apparatus equipped with a Cahn 1000 balance on solid samples. ESR spectra were obtained on powdered samples with a Varian E109 spectrometer operating at X-band frequencies. GC-MS analyses were carried out with an HP5890 gas chromatograph fitted with a 25 m, (3  $\mu\text{m}$ ), PS255 capillary column coupled with a HP5971A MSD instrument.

The  $\text{O}_2$ -uptake measurements were carried out in pyridine with a thermostated gas-volumetric buret system. Repeated experiments showed a reproducibility in the measurements within  $\pm 3\%$ .

Thermogravimetric analyses were obtained under nitrogen atmosphere with a Mettler TA4000 system.

Elemental analyses were carried out at the Microanalytical Laboratory of this university (C, H, N) and at Mikroanalytisches Labor Pascher, Remagen, Germany (Cu, O).

**Synthesis of  $[\text{Cu}_8(\text{dmpz})_8(\text{OH})_8]$  (**2**).** A suspension of  $[\text{Cu}(\text{dmpz})]_n$  (0.85 g, 5.36 mmol) in  $\text{CH}_2\text{Cl}_2$  (100 mL) saturated with water was kept under stirring in a dioxygen atmosphere for 5 days at room temperature. During this time a blue solution formed. The solution was filtered off to remove the unreacted copper(I) complex and evaporated to dryness in vacuo ( $10^{-2}$  Torr) to yield a blue solid (yield ca. 95%). Shorter reaction times were obtained by adding pyridine to the previous reaction system or by carrying out the oxidation in pure pyridine. In a typical preparation,  $[\text{Cu}(\text{dmpz})]_n$  (0.98 g, 6.18 mmol) was added to pyridine (40 mL) containing 0.5 mL of water. The suspension was stirred under dioxygen overnight, obtaining a blue solution, which was evaporated to dryness. The residue was treated with diethyl ether (10 mL), filtered off, washed with diethyl ether and *n*-hexane, and dried in vacuo giving  $[\text{Cu}_8(\text{dmpz})_8(\text{OH})_8] \cdot 2\text{py}$  (yield 90%). Anal. Calcd for  $\text{C}_{50}\text{H}_{74}\text{Cu}_8\text{N}_{18}\text{O}_8$ :

**Table I.** Crystallographic Data for  $[\text{Cu}_8(\text{OH})_8(\text{dmpz})_8] \cdot 2\text{C}_6\text{H}_5\text{NO}_2$  (**2**)

formula	$\text{C}_{52}\text{H}_{74}\text{Cu}_8\text{N}_{18}\text{O}_{12}$	cell vol, $\text{\AA}^3$	4001 (2)
fw	1651.6	Z	2
cryst syst	monoclinic	$D_{\text{calc}}$ , $\text{g cm}^{-3}$	1.371
space group	$P2_1/m$ (No. 11)	wavelength, $\text{\AA}$	0.71073
a, $\text{\AA}$	10.229 (3)	temp, $^\circ\text{C}$	$22 \pm 2$
b, $\text{\AA}$	27.217 (2)	linear abs coeff, $\text{cm}^{-1}$	21.47
c, $\text{\AA}$	14.532 (1)	R	0.064
$\beta$ , deg	98.51 (1)	$R_w$	0.092

C, 38.41; H, 4.74; Cu, 32.52; N, 16.13; O, 8.19. Found: C, 38.33; H, 4.79; Cu, 32.47; N, 16.15; O, 8.11. Mp: 160  $^\circ\text{C}$  dec. Reproducible elemental analyses were not obtained when  $\text{CH}_2\text{Cl}_2$  was used as the reaction medium (see Results and Discussion). The reaction can also be carried out in nitrobenzene by employing a similar procedure,  $[\text{Cu}_8(\text{dmpz})_8(\text{OH})_8] \cdot 2\text{C}_6\text{H}_5\text{NO}_2$  being obtained. Attempts to grow crystals suitable for X-ray studies from dichloromethane or pyridine solutions containing **2** failed owing to the loss of solvent of crystallization. Crystals suitable for X-ray analysis were, however, obtained by recrystallization from nitrobenzene.  $[\text{Cu}_8(\text{pz})_8(\text{OH})_8]$  was prepared from  $[\text{Cu}(\text{pz})]_n$  by using similar experimental conditions. Anal. Calcd for  $\text{C}_{34}\text{H}_{42}\text{Cu}_8\text{N}_{18}\text{O}_8$ : C, 30.49; H, 3.14; Cu, 37.97; N, 18.83; O, 9.57. Found: C, 30.64; H, 3.09; Cu, 37.72; N, 18.16; O, 9.63. Mp: 188  $^\circ\text{C}$  dec.

**Synthesis of  $[\text{Cu}_8(\text{dmpz})_8(\text{OR}')_8]$  (**3**) ( $\text{R}' = \text{Me, Et, Pr}^n, \text{Allyl}$ ).** A suspension of **2** (0.30 g, 0.21 mmol) in methanol (30 mL) was stirred for 8 h at room temperature. The resulting green product was filtered off under a dry nitrogen atmosphere to prevent contamination from moisture, washed with methanol, and dried in vacuo. Anal. Calcd for  $\text{C}_{48}\text{H}_{80}\text{Cu}_8\text{N}_{16}\text{O}_8$ : C, 37.99; H, 5.28; Cu, 33.51; N, 14.78; O, 8.44. Found: C, 37.83; H, 5.34; N, 14.81; O, 8.52. Mp: 177  $^\circ\text{C}$  dec. The reaction of **2** with other alcohols was analogously performed. Complex **2** can be reobtained by stirring suspensions of complexes **3** in wet diethyl ether.

**Stoichiometric Oxygenation of  $\text{PPh}_3$ .** The stoichiometry of the oxygenation of triphenylphosphine to triphenylphosphine oxide was determined by carrying out several reactions with different molar ratios  $\text{PPh}_3/[\text{Cu}_8(\text{dmpz})_8(\text{OH})_8]$  and measuring the amount of  $[\text{Cu}(\text{dmpz})]_n$  obtained (gravimetrically) and the quantity of  $\text{PPh}_3$  and/or  $\text{O}=\text{PPh}_3$  present at the end of the experiment (GC-MS). In a typical run, dinitrogen was bubbled for 30 min through a solution of  $\text{PPh}_3$  in toluene (8 mL). The solution was then thermostated at 60  $^\circ\text{C}$ , and complex **2** (0.30 g, 0.21 mmol) was added under nitrogen. After 6 h the run was stopped, the solution was analyzed, and the insoluble  $[\text{Cu}(\text{dmpz})]_n$  product was filtered off, washed with  $\text{CH}_2\text{Cl}_2$ , dried, and weighed. Only for a ratio of  $\text{PPh}_3/2 = 4$  was all the  $\text{PPh}_3$  converted into  $\text{O}=\text{PPh}_3$ , with a concomitant quantitative yield of  $[\text{Cu}(\text{dmpz})]_n$ . All other runs showed the presence of free  $\text{PPh}_3$  ( $\text{PPh}_3/2 > 4$ ) or an amount of  $[\text{Cu}(\text{dmpz})]_n$  lower than the theoretically predictable amount on the basis of added  $[\text{Cu}_8(\text{dmpz})_8(\text{OH})_8]$  ( $\text{PPh}_3/2 < 4$ ).

**Catalytic Reactions.** In a typical experiment, to a solution of complex **2** (0.012 g,  $8.54 \times 10^{-3}$  mmol) in pyridine (10 mL), thermostated at 60  $^\circ\text{C}$ , was added the organic substrate under a dioxygen atmosphere (ratio of **2**/substrate  $\approx 1/600$ ). The conversion was monitored by sampling periodically the reaction mixture and analyzing by GC-MS. In the case of dibenzylamine, the temperature was set to 90  $^\circ\text{C}$ . The oxidation of CO to  $\text{CO}_2$  was carried out by bubbling carbon monoxide and dioxygen into a solution of complex **2** in pyridine maintained at 60  $^\circ\text{C}$  and trapping the carbon dioxide formed in a solution of  $\text{Ba}(\text{OH})_2$ . A quantitative determination of  $\text{BaCO}_3$  yielded (after 5 h) 4.31 times more  $\text{CO}_2$  than that expected for the stoichiometric reaction of CO with **2**. To test the ability of **2** in catalyzing the CO oxidation also in the solid state, a U-shaped glass tube, approximately 5 mm in diameter, was partially filled with powdered **2** and then heated up to ca. 100  $^\circ\text{C}$ . A constant flow of CO was maintained for about 6 h, and the outgoing gas was bubbled in  $\text{CO}_2$  trap (as described above). No detectable conversion was however measured.

**Reaction of **2** with Cyclohexyl Isocyanide.** To a solution of **2** (0.25 g, 0.18 mmol) in  $\text{CH}_2\text{Cl}_2$  (10 mL) maintained at 40  $^\circ\text{C}$  was added cyclohexyl isocyanide (0.12 g, 1.1 mmol) under dinitrogen. After 8 h of stirring, the resulting pale yellow solution was evaporated to dryness and the oily residue treated with *n*-pentane, giving a white solid (a mixture of  $[\text{Cu}(\text{dmpz})(\text{RNC})]_2$  (**A**) and  $[(\text{RNC})_2\text{Cu}(\text{dmpz}-\text{C}(\text{O})-\text{NR})]$  (**B**) ( $\text{R} = \text{cyclohexyl}$ , vide infra and Scheme II)). Complexes **A** and **B** were separated by exploiting their different solubilities in toluene, and their nature was confirmed by comparing their IR spectra with those of authentic samples.<sup>5</sup>

**Collection and Reduction of X-ray Data.** A blue prismatic crystal of dimensions  $0.25 \times 0.15 \times 0.10$  mm was selected and mounted on a glass

- (3) Karlin, K. D.; Gultneh, Y. In *Progress in Inorganic Chemistry*; Lippard, J., Ed.; Wiley: New York, 1987, Vol. 35, p 219.
- (4) Hulsbergen, F. B.; ten Hoedt, R. W. H.; Verschoor, G. C.; Reedijk, J.; Spek, A. L. *J. Chem. Soc., Dalton Trans.* **1983**, 539 and references therein.
- (5) (a) Ardizzoia, G. A.; La Monica, G.; Angaroni, M. A.; Cariati, F. *Inorg. Chim. Acta* **1989**, *158*, 159. (b) Ardizzoia, G. A.; Angaroni, M. A.; La Monica, G.; Masciocchi, N.; Moret, M. *J. Chem. Soc., Dalton Trans.* **1990**, 2277.
- (6) (a) Ardizzoia, G. A.; Angaroni, M. A.; La Monica, G.; Cariati, F.; Moret, M.; Masciocchi, N. *J. Chem. Soc., Chem. Commun.* **1990**, 1021; (b) Ardizzoia, G. A.; Angaroni, M. A.; La Monica, G.; Cariati, F.; Cenini, S.; Moret, M.; Masciocchi, N. *Abstracts of Papers*, VIII International Symposium on Homogeneous Catalysis, Lyon, 1990; P67.
- (7) (a) Okkersen, H.; Groeneveld, W. L.; Reedijk, J. *Recl. Trav. Chim. Pays-Bas* **1973**, *92*, 945. (b) Singh, C. B.; Satpathy, S.; Sahoo, B. *J. Inorg. Nucl. Chem.* **1971**, *33*, 1313.

**Table II.** Fractional Atomic Coordinates and Their Estimated Standard Deviations for Non-Hydrogen Atoms of [Cu<sub>8</sub>(OH)<sub>8</sub>(dmpz)<sub>8</sub>·2C<sub>6</sub>H<sub>5</sub>NO<sub>2</sub> (2)

atom	x/a	y/b	z/c
Cu1	0.0006 (2)	0.3090 (1)	-0.3126 (2)
Cu2	0.0642 (2)	0.3894 (1)	-0.1466 (2)
Cu3	0.1269 (2)	0.38942 (9)	0.0805 (2)
Cu4	0.1627 (2)	0.30906 (9)	0.2475 (2)
O1	-0.106 (2)	0.250	-0.327 (1)
O2	0.123 (1)	0.3555 (5)	-0.2479 (8)
O3	0.002 (1)	0.3997 (5)	-0.0289 (8)
O4	0.244 (1)	0.3560 (5)	0.1756 (8)
O5	0.072 (2)	0.250	0.274 (1)
N1	0.129 (1)	0.2251 (5)	-0.3777 (9)
N2	-0.139 (1)	0.3535 (6)	-0.287 (1)
N3	-0.111 (1)	0.3883 (6)	-0.219 (1)
N4	0.240 (1)	0.4106 (5)	-0.085 (1)
N5	0.269 (1)	0.4100 (5)	0.011 (1)
N6	-0.009 (1)	0.3872 (6)	0.1654 (9)
N7	0.010 (1)	0.3524 (5)	0.2356 (9)
N8	0.327 (1)	0.2249 (5)	0.2947 (9)
C1	0.242 (2)	0.156 (1)	-0.444 (2)
C2	0.217 (2)	0.2087 (7)	-0.431 (1)
C3	0.271 (3)	0.250	-0.466 (2)
C4	-0.324 (2)	0.329 (1)	-0.411 (2)
C5	-0.260 (2)	0.3618 (9)	-0.330 (1)
C6	-0.311 (2)	0.402 (1)	-0.294 (1)
C7	-0.214 (2)	0.4155 (8)	-0.225 (1)
C8	-0.218 (2)	0.460 (1)	-0.168 (2)
C9	0.348 (2)	0.4353 (8)	-0.220 (1)
C10	0.343 (2)	0.4275 (7)	-0.118 (1)
C11	0.439 (2)	0.4396 (7)	-0.048 (1)
C12	0.386 (2)	0.4277 (7)	0.032 (1)
C13	0.452 (2)	0.4311 (8)	0.130 (2)
C14	-0.159 (2)	0.4548 (9)	0.108 (1)
C15	-0.112 (2)	0.4136 (7)	0.174 (1)
C16	-0.167 (2)	0.3969 (7)	0.251 (1)
C17	-0.091 (2)	0.3606 (7)	0.286 (1)
C18	-0.099 (2)	0.3295 (9)	0.367 (2)
C19	0.478 (2)	0.1562 (9)	0.346 (1)
C20	0.449 (2)	0.2102 (8)	0.334 (1)
C21	0.525 (2)	0.250	0.358 (2)
O6	-0.439 (2)	-0.0334 (8)	-0.574 (1)
O7	-0.386 (2)	0.0441 (8)	-0.612 (1)
N9	-0.376 (2)	0.0053 (7)	-0.570 (1)
C22	-0.257 (2)	0.0063 (8)	-0.492 (1)
C23	-0.167 (2)	0.0438 (9)	-0.488 (2)
C24	-0.244 (2)	-0.0320 (9)	-0.433 (2)
C25	-0.127 (2)	-0.033 (1)	-0.361 (2)
C26	-0.040 (2)	0.002 (1)	-0.354 (2)
C27	-0.055 (2)	0.042 (1)	-0.412 (2)

fiber tip onto a goniometer head. Single-crystal X-ray diffraction data were collected on an Enraf-Nonius CAD4 diffractometer with the use of graphite-monochromatized Mo K $\alpha$  radiation ( $\lambda = 0.71073 \text{ \AA}$ ). The unit cell parameters were determined by using the setting angles of 25 randomly distributed intense reflections having  $10^\circ < \theta < 14^\circ$ . Crystal data are summarized in Table I. No crystal decay was observed under the experimental conditions. The observed intensities were corrected for Lorentz and polarization effects and reduced to  $F_o$ . An empirical absorption correction was applied as described in ref 8 by using  $\psi$  scans of three suitable reflections having  $\chi$  values near  $90^\circ$ . From systematic absences ( $0k0$ ,  $k = 2n + 1$ ), the centrosymmetric space group  $P2_1/m$  (No. 11) was originally assumed and later confirmed by successful solution and refinement of the structure. Of the 5672 reflections collected in the  $\pm h, k, l$  octants, 2185 (with  $I > 3\sigma(I)$ ) were subsequently used for structure solution and refinement.

**Solution and Refinement of the Structure.** The positions of the four independent copper atoms were obtained from direct methods (MULTAN<sup>8</sup>), and the remaining lighter O, N, and C atoms were located from subsequent difference Fourier syntheses. The hydrogen atoms of the pyrazole ligands were included in the last stages of the refinement in idealized positions ( $C-H = 0.95 \text{ \AA}$ ,  $B_{iso} = 5.0 \text{ \AA}^2$ ). Anisotropic thermal

**Table III.** Relevant Bond Distances ( $\text{\AA}$ ) and Their Estimated Standard Deviations in the [Cu<sub>8</sub>(dmpz)<sub>8</sub>(OH)<sub>8</sub>] Molecule (2)<sup>a</sup>

individual		average	
Cu1-Cu1'	3.211 (4)	Cu-Cu	3.238
Cu1-Cu2	3.251 (3)		
Cu2-Cu3	3.268 (2)		
Cu3-Cu4	3.247 (2)		
Cu4-Cu4'	3.215 (4)		
Cu1-O1	1.934 (8)	Cu-O	1.920
Cu1-O2	1.924 (9)		
Cu2-O2	1.908 (9)		
Cu2-O3	1.932 (8)		
Cu3-O3	1.907 (8)		
Cu3-O4	1.919 (8)		
Cu4-O4	1.917 (9)		
Cu4-O5	1.923 (6)		
N1-N1'	1.36 (2)	N-N	1.37
N2-N3	1.36 (1)		
N4-N5	1.38 (1)		
N6-N7	1.38 (1)		
N8-N8'	1.36 (2)		
N1-C2	1.35 (1)	N-C	1.32
N2-C5	1.32 (2)		
N3-C7	1.28 (2)		
N4-C10	1.31 (1)		
N5-C12	1.28 (1)		
N6-C15	1.30 (1)		
N7-C17	1.36 (1)		
N8-C20	1.36 (1)		
C2-C3	1.38 (2)	C=C	1.36
C5-C6	1.36 (2)		
C6-C7	1.35 (2)		
C10-C11	1.35 (2)		
C11-C12	1.39 (2)		
C15-C16	1.39 (2)		
C16-C17	1.31 (2)		
C20-C21	1.35 (2)		
C1-C2	1.48 (2)	C-C	1.49
C4-C5	1.55 (3)		
C7-C8	1.47 (3)		
C9-C10	1.50 (2)		
C12-C13	1.48 (2)		
C14-C15	1.50 (2)		
C17-C18	1.46 (2)		
C19-C20	1.50 (2)		

<sup>a</sup> Primed atoms refer to the  $x$ ,  $-y$ ,  $z$  symmetry operation equivalent.

parameters were assigned to all the atoms of the octameric molecule, while the atoms of the clathrated nitrobenzene molecule were given isotropic  $B$ 's. Full-matrix least-squares refinement of 367 variables converged to  $R$ ,  $R_w$ , and GOF factors of 0.064, 0.092, and 2.232, the minimized function being  $\sum w(|F_o| - k|F_c|)^2$ . Individual weights were assigned as  $w = 1/\sigma^2(F_o)$ , where  $\sigma(F_o) = \sigma(F_o^2)/2F_o$ ,  $\sigma(F_o^2) = [\sigma^2(I) + (pI)^2]^{1/2}/L_p$ , where  $L_p$  is the Lorentz-polarization factor and  $p$ , the ignorance factor, was set at 0.04. Owing to the presence of highly disordered molecules within the holes (or channels) of the crystal lattice, several significant peaks, not exceeding  $1.5 \text{ e/\AA}^3$ , in the last residual Fourier maps were found, but their geometry could not be rationalized. Scattering factors, corrected for real and imaginary anomalous dispersion terms, were taken from ref 10. All computations were performed on a PDP 11/73 computer, using the Enraf-Nonius SDP package.<sup>11</sup> Final atomic coordinates with the estimated standard deviations are presented in Table II. Selected interatomic distances and bond angles, together with their estimated standard deviations, are given in Table III and IV, respectively.

## Results and Discussion

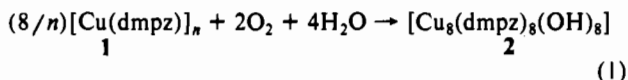
[Cu(dmpz)]<sub>n</sub> (1) reacts quantitatively in wet dichloromethane with molecular oxygen at room temperature to form the octanuclear complex [Cu<sub>8</sub>(dmpz)<sub>8</sub>(OH)<sub>8</sub>] (2) (eq 1).

(8) North, A. C. T.; Phillips, D. C.; Mathews, F. S. *Acta Crystallogr. Sect. A* 1968, 24, 351.

(9) Germain, G.; Main, P.; Woolson, M. M. MULTAN, a system of computer programs for the automatic solution of crystal structures from X-ray diffraction data. *Acta Crystallogr., Sect. A* 1971, A27, 368.

(10) *International Tables for X-Ray Crystallography*; Kynoch Press: Birmingham, England, 1974; Vol. 4.

(11) Frenz, B. A. and Associates, *SDP Structure Determination Package Plus, Version 1.0*; Enraf-Nonius: Delft, The Netherlands 1980.

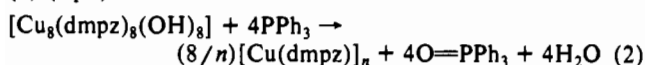


Analogously,  $[\text{Cu}(\text{pz})]_n$  (Hpz = pyrazole) gives the corresponding  $[\text{Cu}_8(\text{pz})_8(\text{OH})_8]$  under identical experimental conditions.

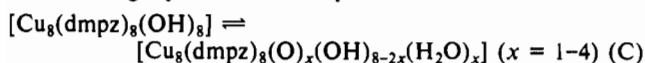
The presence of free water was confirmed to be necessary in order to obtain **2** or  $[\text{Cu}_8(\text{pz})_8(\text{OH})_8]$ . Repeated  $\text{O}_2$ -uptake measurements always gave a Cu/ $\text{O}_2$  ratio equal to 4.

Reaction 1 can be carried out also in pyridine or nitrobenzene. In these cases, complex **2** was recovered containing 2 mol of clathrated pyridine or nitrobenzene/mol of octameric unit. When obtained in wet  $\text{CH}_2\text{Cl}_2$ , complex **2** was shown to contain clathrated water (spectroscopic and analytical evidences). In the latter case, we did not succeed in having reproducible elemental analyses, owing to the presence of variable amounts of water. Reaction times were confirmed to be related to the nature of the solvent, a faster reaction being observed when pyridine was used. This fact could be attributed to the capability of this nitrogen ligand to solubilize the starting polymeric  $[\text{Cu}(\text{dmpz})]_n$  (**1**). The IR spectrum of **2**, obtained from  $\text{CH}_2\text{Cl}_2$  (Nujol mull or KBr pellets), exhibits absorptions that confirmed the presence of bridging OH groups [ $\nu(\text{OH}) = 3637$  s and  $3598$  s  $\text{cm}^{-1}$ ].<sup>12</sup> Moreover, two bands at  $3392$  s, br and  $898$  vs  $\text{cm}^{-1}$  are present. On the basis of literature data,<sup>13a</sup> we assign these absorptions to  $\nu(\text{OH})$  and libration of clathrated water molecules (vide infra). On treatment with  $\text{D}_2\text{O}$ , the above bands shift to  $2673$  s,  $2645$  s,  $2532$  m, br, and  $647$  m  $\text{cm}^{-1}$ ; isotopic shifts are in agreement with analogous results already published.<sup>13</sup> The latter two absorptions were absent in the IR spectrum of complex **2** recovered from pyridine, after pumping to constant weight. Thermogravimetric analysis of complex **2** did not show separate peaks for loss of the clathrated solvent molecules and decomposition processes; instead, only a continuous slope, starting at ca.  $100^\circ\text{C}$ , was observed. The magnetic moment of complex **2** at room temperature gave a value of  $2.10 \mu_B$  per octameric unit. This value decreases with decreasing temperature,  $1.17 \mu_B$  being found at  $77$  K. This fact indicates strong exchange coupling between the metals in the octamer. Moreover, the ESR spectra of **2**, recorded at room and at liquid-nitrogen temperatures (powdered sample), as well as in frozen  $\text{CH}_2\text{Cl}_2$  solution, showed only a very weak signal at ca.  $3000$  G ( $1$  G =  $10^{-4}$  T). The origin of this signal, which may also arise from contamination from paramagnetic impurities (very common in antiferromagnetic materials), and a detailed study of the magnetic properties of compound **2** are presently under investigation.

**Stoichiometry of Oxidation of  $\text{PPh}_3$  by **2** under  $\text{N}_2$ .** Complex **2** showed an unexpected behavior when reacted with excess triphenylphosphine at  $60^\circ\text{C}$  under an inert atmosphere. Four moles of  $\text{O}=\text{PPh}_3$  per mole of **2** were obtained, while the metal was recovered in a quantitative yield as the polymeric  $[\text{Cu}(\text{dmpz})]_n$  (**1**) (eq 2).



This behavior can be explained by assuming that, in solution, the following equilibrium takes place:



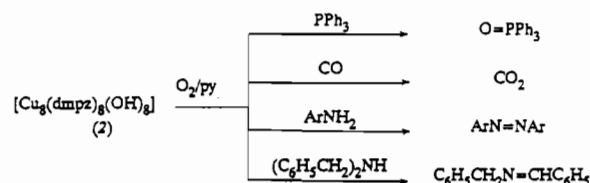
The tautomeric species (C) are the plausible active species in the phosphine oxidation. The existence of species C is suggested by preliminary results from variable-temperature  $^1\text{H}$  NMR ( $\text{CD}_2\text{Cl}_2$  solution), which showed the presence of two peaks merging above  $0^\circ\text{C}$  ( $\delta = 14.7$  and  $\delta = 16.5$  ppm at  $-80^\circ\text{C}$ ); while the pyrazolate proton resonances appear virtually unchanged at all temperatures, we attribute these low-field signals to OH and  $\text{H}_2\text{O}$  protons. A detailed NMR study to clarify the nature of these

**Table IV.** Relevant Bond Angles (deg) and Their Estimated Standard Deviations in the  $[\text{Cu}_8(\text{dmpz})_8(\text{OH})_8]$  Molecule (**2**)<sup>a</sup>

individual		average	
O1-Cu1-O2	156.0 (5)	O-Cu-O	158.3
O2-Cu2-O3	159.3 (4)		
O3-Cu3-O4	160.0 (4)		
O4-Cu4-O5	158.0 (5)		
O1-Cu1-N1	87.8 (5)	O-Cu-N <sub>endo</sub>	87.3
O2-Cu2-N3	86.8 (5)		
O3-Cu3-N5	89.2 (4)		
O4-Cu4-N7	87.5 (4)		
O2-Cu1-N2	85.5 (5)		
O3-Cu2-N4	87.3 (4)		
O4-Cu3-N6	87.5 (4)		
O5-Cu4-N8	87.1 (4)		
O1-Cu1-N2	96.8 (5)	O-Cu-N <sub>exo</sub>	95.7
O2-Cu2-N4	97.0 (4)		
O3-Cu3-N6	94.5 (4)		
O4-Cu4-N8	95.0 (4)		
O2-Cu1-N1	96.6 (4)		
O3-Cu2-N3	94.9 (4)		
O4-Cu3-N5	94.3 (4)		
O5-Cu4-N7	96.8 (4)		
N1-Cu1-N2	161.4 (5)	N-Cu-N	163.0
N3-Cu2-N4	163.3 (5)		
N5-Cu3-N6	164.1 (5)		
N7-Cu4-N8	163.2 (4)		
Cu1-O1-Cu1'	112.2 (7)	Cu-O-Cu	114.8
Cu1-O2-Cu2	116.1 (4)		
Cu2-O3-Cu3	116.7 (4)		
Cu3-O4-Cu4	115.7 (4)		
Cu4-O5-Cu4'	113.5 (6)		
		Cu-N-N	118.5
		Cu-N-C	134.0
		N-N-C	107.3
		N-C-C <sub>endo</sub>	110
		N-C-C <sub>exo</sub>	121
		C-C-C <sub>endo</sub>	106

<sup>a</sup>The endo and exo subscripts refer to the five-membered rings to which they belong. Primed atoms refer to the  $x$ ,  $-y$ ,  $z$  symmetry operation equivalent.

#### Scheme I



equilibria is in progress. Protonic transfer from **2** to solvent molecules, competing with intramolecular pathways (generating C), are, in our opinion, unlikely, based on the observation that the oxygen transfer takes place in a variety of solvents of different donor properties (pyridine, toluene, halocarbons).

It is well known that oxo-bridged dimeric Cu(II) complexes are able to transfer an oxygen atom to  $\text{PPh}_3$  to give  $\text{O}=\text{PPh}_3$ .<sup>3</sup> Moreover, oxidation and oxygenation reactions of external substrates other than  $\text{PPh}_3$  (carbon monoxide, cyclohexyl isocyanide, etc.), under a dinitrogen atmosphere, were observed in the presence of complex **2**, although no quantitative measurements were performed (see below).

**Catalytic Properties of **2**.** When reaction 2 has been carried out in pyridine at  $60^\circ\text{C}$  under a dioxygen atmosphere, the catalytic formation of  $\text{O}=\text{PPh}_3$  was observed (Scheme I). After 6 h, with a concentration of **2** of about  $3 \times 10^{-3}$  mol  $\text{L}^{-1}$ ,  $0.41$  mol of  $\text{PPh}_3$  were converted into triphenylphosphine oxide.

It must be pointed out that pyridine was shown to be essential in order to have reaction 2 proceed in a catalytic fashion. This is related to the fact, already mentioned, that only in this solvent is  $[\text{Cu}(\text{dmpz})]_n$  (**1**), formed in reaction 2, soluble enough to allow its ready reoxidation leading to the octameric complex **2** (eq 2).

(12) Jones, L. H. *J. Chem. Phys.* **1954**, *22*, 217.

(13) (a) Adams, D. M.; Cook, P. J. *J. Chem. Soc. A* **1971**, 2801. (b) Falk, M.; Knop, O. *Can. J. Chem.* **1977**, *55*, 1736. (c) Thomas, G. H.; Falk, M.; Knop, O. *Can. J. Chem.* **1974**, *52*, 1029.

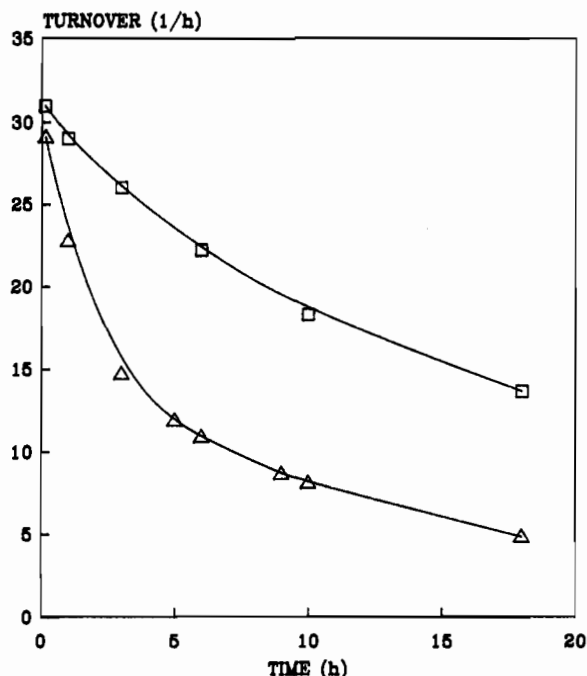


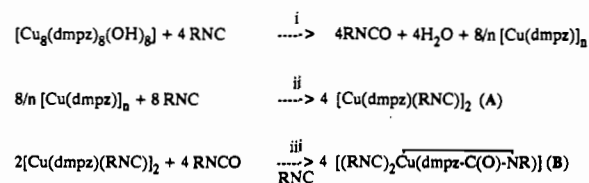
Figure 1. Turnover ( $[\text{substrate}]/[(2)](\text{time})$ ) vs time (h) for PPh<sub>3</sub> (□) and (C<sub>6</sub>H<sub>5</sub>CH<sub>2</sub>)<sub>2</sub>NH (Δ) catalytic oxidations.

Carbon monoxide and aromatic amines (aniline, *p*-toluidine) are converted under similar experimental conditions, into carbon dioxide and azobenzenes, respectively (Scheme I). In the latter case, azobenzenes were confirmed to be the only product of the catalytic oxidative coupling reaction. Although reactions of metal oxo complexes with CO to generate CO<sub>2</sub> have already been reported,<sup>14</sup> to our knowledge there is no mention in the literature of homogeneous copper catalysts of this type. Attempts to perform the catalytic oxidation of CO, by flowing the gas on a bed of solid 2, failed (see Experimental Section).

The utility of [Cu<sub>8</sub>(dmpz)<sub>8</sub>(OH)<sub>8</sub>] (2) as a selective catalyst was verified in the oxidation reaction of a secondary amine such as (C<sub>6</sub>H<sub>5</sub>CH<sub>2</sub>)<sub>2</sub>NH. This substrate can be converted into *N*-benzylidenebenzylamine, C<sub>6</sub>H<sub>5</sub>CH<sub>2</sub>N=CHC<sub>6</sub>H<sub>5</sub>, with a high selectivity (ca. 99%). Among the observed byproducts, benzaldehyde, derived from the hydrolysis reaction of the Schiff base, was shown to be the main product. It is worth noticing that the activity of our catalytic system decreases with time. Figure 1 shows the change of the turnover vs time for PPh<sub>3</sub> and (C<sub>6</sub>H<sub>5</sub>CH<sub>2</sub>)<sub>2</sub>NH oxidation reactions. Moreover, the decreasing of the catalytic activity was shown to be sensitive to the reaction temperature. In fact, in the case of PPh<sub>3</sub> oxidation, which requires a lower temperature, the catalyst's life was longer (see Experimental Section). Finally, we confirmed that the catalyst's life was longer also in the oxidation reaction of (C<sub>6</sub>H<sub>5</sub>CH<sub>2</sub>)<sub>2</sub>NH, provided that it is carried out in two steps: (a) oxidation of the substrate at 90 °C in pyridine under dinitrogen; (b) reoxidation of the formed [Cu(dmpz)]<sub>n</sub> (1) at room temperature. The observed decreasing of the catalytic activity is most probably related to the partial irreversible oxidation of [Cu(dmpz)]<sub>n</sub> to give copper(II) products, which has been verified during our catalytic reactions; however, we were unable to ascertain the nature of these products.

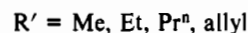
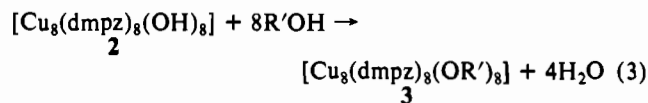
**Oxidation Reaction of Cyclohexyl Isocyanide by 2.** Cyclohexyl isocyanide (RNC) was converted into the corresponding isocyanate when reacted with 2 under an inert atmosphere (Scheme II, reaction i). We did not succeed in isolating RNCO as a free species, it being readily involved in a subsequent reaction (Scheme II, reaction iii). The already reported<sup>5b</sup> [Cu(dmpz)(RNC)]<sub>2</sub> (A) and [(RNC)<sub>2</sub>Cu(dmpz-C(O)-NR)] (B) were shown to be the

#### Scheme II



only reaction products. Moreover, the IR spectrum of the reaction solution did not show any absorption assignable to the presence of free RNCO. Complexes A and B were recently obtained by us by performing reactions ii and iii (Scheme II).<sup>5b</sup> The stoichiometric conversion of RNC into RNCO was again observed when dioxygen was present. Also in this case, the final reaction products were the copper(I) derivatives A and B. Finally, it has been recently verified that both complexes A and B do not react with dioxygen if free cyclohexyl isocyanide is present in the reaction medium. On the other hand, a facile reaction was observed between complex A and dioxygen only in the absence of free RNC.<sup>15</sup> The nature of the reaction product is at the moment unknown.

**Reactions of 2 with Aliphatic Alcohols.** [Cu<sub>8</sub>(dmpz)<sub>8</sub>(OH)<sub>8</sub>] (2) reacts with aliphatic alcohols, giving green Cu(II)-octaalkoxo derivatives (eq 3).



Their formation is achieved only by using excess alcohols. The formulation of complexes 3 as octameric species is essentially based on the observation that they are sensitive to moisture, even in the solid state, complex 2 being reobtained. This behavior could not be easily explained if major rearrangements leading to the octameric unit were required.

The IR spectra of 3 did not show any absorption due to  $\nu(\text{OH})$  in the 3200–3600-cm<sup>-1</sup> region, while bands assignable to alkoxo groups were detected (1050–1100-cm<sup>-1</sup> region). The rate of the reverse reactions giving 2 were shown to be related to the nature of the R' (Me > Et > Pr<sup>n</sup> ≈ allyl).

Attempts are in due course to grow crystals suitable for an X-ray investigation; so far reasonably diffracting crystals have been obtained for the Pr<sup>n</sup> and the allyl derivatives, but their stability under diffraction conditions, even in glass capillaries with their mother liquors, was poor and prevented any data collection.

It must be pointed out that no reaction was observed when 2 was treated with secondary or tertiary alcohols. This behavior seems to suggest that steric effects play an important role in the reactivity of complex 2 (vide infra). Similarly, it was observed that *tert*-butyl isocyanide failed in its conversion into the corresponding isocyanate.

**Description of the Structure.** The crystals of [Cu<sub>8</sub>(dmpz)<sub>8</sub>(OH)<sub>8</sub>]<sub>2</sub>C<sub>6</sub>H<sub>5</sub>NO<sub>2</sub> consist of a molecular packing of discrete [Cu<sub>8</sub>(dmpz)<sub>8</sub>(OH)<sub>8</sub>] molecules and clathrated nitrobenzene molecules in a 1:2 molar ratio, exhibiting normal van der Waals contacts.

The molecular structure of [Cu<sub>8</sub>(dmpz)<sub>8</sub>(OH)<sub>8</sub>], which lies on a crystallographic mirror plane (*e* in Wyckoff notation), can be described in terms of a cyclic sequence of eight (almost identical) monomeric units giving rise to a peculiar toroidal shape of idealized *D*<sub>4d</sub> symmetry. Figure 2a shows an ORTEP drawing of the [Cu<sub>8</sub>(dmpz)<sub>8</sub>(OH)<sub>8</sub>] molecule viewed down the pseudo-8-fold rotary inversion *S*<sub>8</sub> axis.

The eight metal atoms, which lie approximately at the vertices of a regular octagon (maximum displacement from the "best" Cu<sub>8</sub> plane = 0.013 (2) Å), are connected by  $\mu$ -bridging OH and dmpz

(14) Kim, Y.; Gallucci, J.; Wojcicki, A. *J. Am. Chem. Soc.* **1990**, *112*, 8600 and references therein.

(15) Ardizzoia, G. A.; Angaroni, M. A.; La Monica, G.; Moret, M.; Masciocchi, N. Unpublished results.

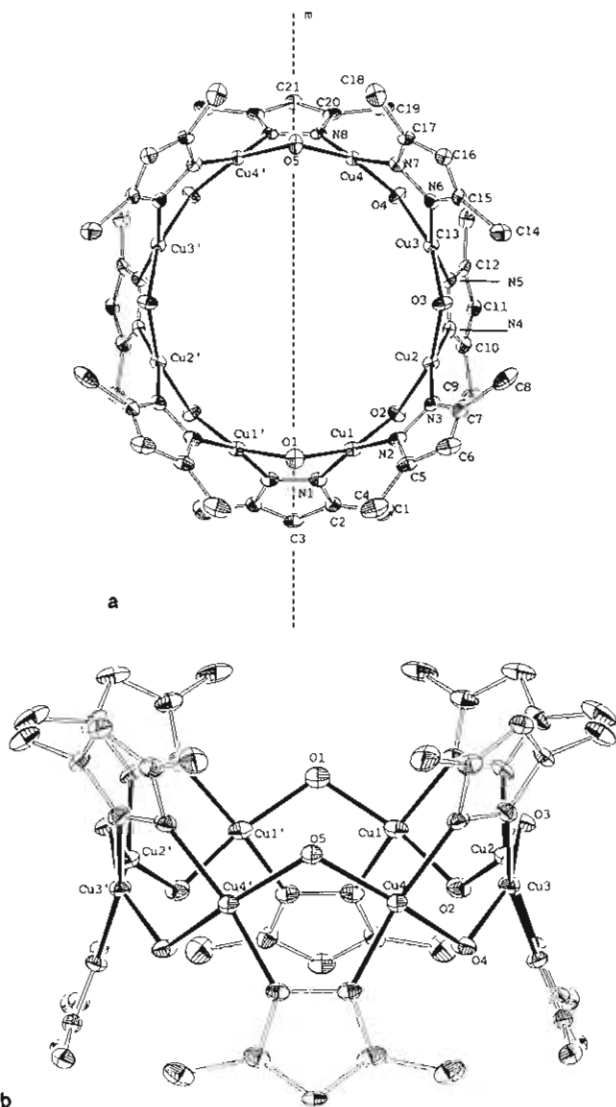


**Figure 2.** ORTEP<sup>23</sup> drawing of the  $[\text{Cu}_8(\text{OH})_8(\text{dmpz})_8]$  molecule, with partial labelling scheme: (a) top view; (b) side view. Thermal ellipsoids have been drawn at 30% probability. For sake of clarity, hydrogen atoms have been omitted.

ligands in an alternate "up and down" sequence; this arrangement of spiro  $\text{Cu-O-Cu-N-N}$  five-membered rings generates a ribbon of trans, roughly square-planar copper complexes, which surrounds the central cavity. The average nonbonding distance for adjacent copper atoms, 3.238 Å (minimum 3.213, maximum 3.268 Å), is comparable with those found in  $[\text{Cu}_3(\text{pz})_3(\text{C}_5\text{H}_5\text{N})_2(\text{OH})\text{Cl}_2] \cdot \text{C}_5\text{H}_5\text{N}$ <sup>16</sup> and  $[\text{Cu}_3(\text{pz})_3(\text{Hpz})_2(\text{OH})(\text{NO}_3)_2] \cdot \text{H}_2\text{O}$ <sup>4</sup> (minimum 3.11 Å; maximum 3.36 Å), but shorter than those of other polynuclear pyrazolate-bridged copper compounds not containing hydroxo bridges, such as  $[\text{Cu}(\text{dmpz})(\text{RNC})]_2$ <sup>5b</sup> and  $[\text{Cu}(\text{dcmpz})(\text{RNC})]_2$ <sup>15</sup> (Hdcmpz = 3,5-dicarbomethoxypyrazole), 3.56 and 3.40 Å, respectively. A recent X-ray study of  $[\text{Cu}(\text{dppz})_4]$ <sup>15</sup> (Hdppz = 3,5-diphenylpyrazole) showed however Cu-Cu nonbonding interactions as low as 3.088 (1) Å.

Owing to the strict similarity of the refined bond distances and angles of the four crystallographically independent monomers, the following discussion, when not differently stated, will deal with an idealized monomeric unit, whose parameters were obtained by averaging chemically equivalent values.

The bond distances between the copper and the lighter (O and N) atoms well compare with those reported for a series of

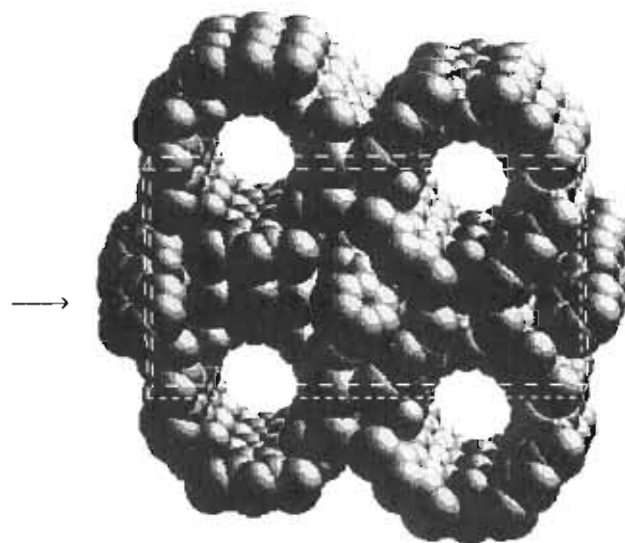


**Figure 3.** Space-filling model, generated with the program SMILE,<sup>24</sup> of the contents of three unit cells, viewed approximately down the crystallographic  $a$  axis. Note the infinite channels originated by the stack of the octameric molecules and the clathrated nitrobenzene molecules (arrow).

analogous compounds. In particular, all the individual Cu-O bond distances (average value 1.920 Å) agree well with the observed values of Cu-OH-Cu systems, rather than those of the few known Cu-O-Cu<sup>17</sup> or Cu-OH<sub>2</sub>-Cu ones;<sup>18</sup> moreover, the thermal ellipsoids of the oxygen atoms (see Figure 2a) do not seem particularly prolated toward the copper atoms, as if they were smoothing out different coordination modes of oxo, hydroxo, or water ligands, thus suggesting that tautomers of general formula  $[\text{Cu}_8(\text{dmpz})_8(\text{O})_x(\text{OH})_{8-2x}(\text{H}_2\text{O})_x]$  ( $x = 1-4$ ) might be of little importance in the solid state.

However, the geometry around the metal center, which is somewhat distorted from idealized square-planar coordination ( $\text{O-Cu-O}$ , 158.3°;  $\text{O-Cu-N}_{\text{endo}}$ , 87.3°;  $\text{O-Cu-N}_{\text{exo}}$ , 95.7°;  $\text{N-Cu-N}$ , 163°; the endo and exo subscripts refer to the spiro  $\text{Cu}_2\text{N}_2$  rings), reflecting therefore the folding of the aforementioned ribbon to achieve a cyclic system, allows the presence

of an envelope conformation of the  $\text{Cu-O-Cu-N-N}$  cycles, similar to those found in the compounds of ref 19, with the oxygen atoms ca. 0.7 Å apart from the best  $\text{Cu}_2\text{N}_2$  planes. The typical dihedral angle between the coordination planes of adjacent copper atoms, 138°, is also consistent with high coupling of the magnetic moments: a similar effect was observed for the trinuclear hydroxo complexes of copper(II) discussed in ref 16.

The pattern of bond distances and angles within the dimethylpyrazolate ligands is regular, and strict planarity of the rings was observed, the maximum deviation from the molecular plane being 0.01 (2) Å. These ligands typically are at an angle of about 120° from the octacopper plane, thus forming a double crown (of four dmpz each) on both sides of the  $[\text{CuON}_2]_8$  ribbon, as depicted in Figure 2b, where a side view of the complex is shown. This hourglass-shaped feature of the molecule, more than the internal cavity, which, after subtraction of proper van der

(16) Angaroni, M. A.; Ardizzoia, G. A.; Beringhelli, T.; La Monica, G.; Gatteschi, D.; Masciocchi, N.; Moret, M. *J. Chem. Soc., Dalton Trans.* **1990**, 3305.

(17) (a) Butcher, R. J.; O'Connor, C. J.; Sinn, E. *Inorg. Chem.* **1981**, *20*, 537. (b) Albert, C. F.; Healy, P. C.; Kildare, J. D.; Raston, C. L.; Skelton, B. W.; White, A. M. *Inorg. Chem.* **1989**, *28*, 1300.  
(18) (a) Chauvel, C.; Giverd, J. J.; Jeannin, Y.; Kahn, O.; Lavigne, G. *Inorg. Chem.* **1979**, *18*, 3015. (b) Chaudhuri, P.; Ventur, D.; Wiegardt, K.; Peters, E. M.; Peters, K.; Simon, A. *Angew. Chem., Int. Ed. Engl.* **1985**, *24*, 58; (c) Porter, L. C.; Doedens, R. *J. Inorg. Chem.* **1985**, *24*, 1006. (d) Muhonnen, H. *Inorg. Chem.* **1986**, *25*, 4692. (e) Tamura, H.; Ogawa, K.; Mori, W. *J. Crystallogr. Spectrosc. Res.* **1989**, *19*, 203.  
(19) (a) Marongiu, G.; Lingafelter, E. C. *Acta Crystallogr.* **1982**, *B38*, 620; (b) Thompson, L. K. *Can. J. Chem.* **1983**, *61*, 57. (c) Thompson, L. K.; Hanson, A. W.; Ravaswamy, B. S. *Inorg. Chem.* **1984**, *23*, 2459. (d) Mandal, S. K.; Woon, T. C.; Thompson, L. K.; Newlands, M. J.; Gabe, E. G. *Aust. J. Chem.* **1986**, *39*, 1007. (e) Thompson, L. K.; Lee, F. L.; Gabe, E. G. *Inorg. Chem.* **1988**, *27*, 39.

Waals radii, is estimated to possess a viable diameter of about 6 Å, might be responsible for the aforementioned stereochemical selectivity in the substitution and oxidation reactions with alcohols and isocyanides, respectively. In fact, the residual electronic density found in the central hole is mostly located in the wider section of the cavity itself and might represent disordered water or other guest molecules, similar to those found in the topological analogues [V<sub>8</sub>O<sub>8</sub>(OMe)<sub>16</sub>(C<sub>2</sub>O<sub>4</sub>)]<sup>2-</sup><sup>20</sup> and [Mo<sub>8</sub>O<sub>16</sub>(OR)<sub>8</sub>(C<sub>2</sub>O<sub>4</sub>)]<sup>2-</sup><sup>21</sup> (R = Me or Et), where, however, charge localization and bond directionality allowed proper detection of the oxalate guest groups.

Four ordered nitrobenzene molecules per unit cell are located between the copper complex units, close to crystallographic inversion centers. It is interesting to note that any attempt to grow single crystals of [Cu<sub>8</sub>(dmpz)<sub>8</sub>(OH)<sub>8</sub>] suitable for X-ray analysis, without using C<sub>6</sub>H<sub>5</sub>NO<sub>2</sub>, failed as if these solvent molecules fit exactly in the lattice of a theoretical [Cu<sub>8</sub>(dmpz)<sub>8</sub>(OH)<sub>8</sub>] crystalline phase, gluing together the octameric units.

The crystal packing, depicted in Figure 3, shows also the relative orientation of the [Cu<sub>8</sub>(dmpz)<sub>8</sub>(OH)<sub>8</sub>] molecules, which form infinite channels, zeolite-like, along the crystallographic *a* axis. Given that the intermolecular interactions between adjacent molecules are mostly given by the dmpz ligands, a similar stacking of the octameric units could also be maintained in the solid-state structures of the alkoxo derivatives, if the aliphatic residues are small enough; this would also explain the fast substitution reactions with water molecules occurring if the crystals are left in (wet) air, as if their "active" surface were enormously increased by the presence of these channels throughout the whole lattice. In particular, following this transformation under a microscope, we observed that the Pr<sup>n</sup> derivative, forming well-crystallized samples, is readily degraded in air and that the crystals transform and suddenly collapse, forming submicrometer powders, in about 15 min, with no evidence of specific surface degradation.

### Conclusions

Our [Cu(dmpz)]<sub>n</sub>/py/O<sub>2</sub> system bears a formal resemblance to the CuCl/py/O<sub>2</sub> one, extensively studied by Davies and co-workers,<sup>22</sup> who were mostly interested in determining the nature

of the initiator of the catalytic coupling of aromatic amines and phenols. Our Cu(II)-pyrazolato system allowed the formation of azobenzenes under mild experimental conditions and with high selectivities. On the other hand, it failed for the coupling of phenols, because of its high sensitivity to acidic species. In fact, when phenol was reacted with complex **2** in pyridine, unidentified Cu(II)-phenoxo products were recovered. Moreover, it is worth noting that Hdmpz itself, when reacted with **2**, gives polymeric copper(II)-pyrazolato species, [Cu(dmpz)<sub>2</sub>]<sub>n</sub>. The preparation of new polynuclear copper(I) complexes having different pyrazole-derived ligands is under investigation, with the aim to have helpful insights into the reaction of molecular oxygen with the metal centers and in particular into the extent of dioxygen reduction. Finally, attention will be paid to the catalytic activity of the oxidation products of the above copper(I) systems.

**Acknowledgment.** This research was supported by the Italian Consiglio Nazionale delle Ricerche (Progetto Finalizzato Chimica Fine II). We are grateful to Dr. Andrea Pozzi for the magnetic measurements.

**Registry No.** **1**, 51344-54-8; **2**, 136536-74-8; 2·2C<sub>6</sub>H<sub>5</sub>NO<sub>2</sub>, 136599-16-1; **3** (R' = Me), 136536-75-9; **3** (R' = Et), 136536-76-0; **3** (R' = Pr<sup>n</sup>), 136536-77-1; **3** (R' = allyl), 136568-74-6; dmpz<sup>-</sup>, 122039-72-9; PPh<sub>3</sub>, 603-35-0; CO, 630-08-0; [Cu(dmpz)(RNC)]<sub>2</sub> (R = cyclohexyl), 122108-99-0; [(RNC)<sub>2</sub>Cu(dmpz-C(O)-NR)] (R = cyclohexyl), 136536-78-2; (C<sub>6</sub>H<sub>5</sub>CH<sub>2</sub>)<sub>2</sub>NH, 103-49-1; C<sub>6</sub>H<sub>5</sub>CH<sub>2</sub>N=CHC<sub>6</sub>H<sub>5</sub>, 780-25-6; cyclohexyl isocyanide, 931-53-3; aniline, 62-53-3; *p*-toluidine, 106-49-0.

**Supplementary Material Available:** A detailed list of crystallographic parameters (Table S1), a full list of bond distances and angles (Table S2), a list of anisotropic and isotropic thermal factors (Table S3), a list of "best" molecular planes formed by selected groups of atoms (Table S5), and a list of fractional coordinates of hydrogen atoms (Table S6) (10 pages); a list of observed and calculated structure factor moduli (Table S4) (9 pages). Ordering information is given on any current masthead page.

(20) Chen, Q.; Liu, S.; Zubieta, J. *Inorg. Chem.* **1989**, *28*, 4434.

(21) Chen, Q.; Liu, S.; Zubieta, J. *Angew. Chem., Int. Ed. Engl.* **1987**, *23*, 378.

- (22) El-Sayed, M. A.; Abu-Ragabah, A.; Davies, G.; El-Toukhy, A. *Inorg. Chem.* **1989**, *28*, 1909 and references therein.
- (23) A Fortran thermal-ellipsoid-plot program for crystal structure illustrations: Johnson, C. K.; ORTEP; Oak Ridge National Laboratory: Oak Ridge, TN, 1971.
- (24) SMILE—shaded molecular imaging on low-cost equipment: Eufri, D.; Sironi, A.; *J. Mol. Graphics* **1989**, *7*, 165.